

EFFECT OF CIRCUIT ARRANGEMENT ON THE PERFORMANCE OF PLATE FINNED TUBE HEAT EXCHANGERS UNDER DEHUMIDIFYING CONDITIONS

Min-Sheng Liu, Jin-Sheng Leu, and Chi-Chuan Wang

Energy & Resources Laboratories,
Industrial Technology Research Institute,
Hsinchu, Taiwan
E-mail: f870999@eri.itri.org.tw

Vince C., Mei

Oak Ridge National Laboratory
Oak Ridge, Tennessee 37830
U.S.A.

ABSTRACT

This study experimentally investigates the effect of circuitry on the performance of plate finned tube evaporators. Experiments were carried out with the heat exchangers having 1-circuit arrangements. A total of six circuitry were examined in this study, including two counter-cross, two parallel-cross, and two z-shape arrangements. The results showed that the counter-cross arrangement gives the best performance. However, heat conduction along the fins may offset the benefits of the counter-cross arrangement. In addition, the pressure drop of refrigerant-side increased with frontal velocities. Among the six 1-circuit arrangements, the parallel-cross flow circuit would produce a larger pressure drop than other arrangements. However, for $G = 200 \text{ kg/m}^2\cdot\text{s}$ and parallel flow, the pressure drops decrease with increase of the frontal velocity. The unusual characteristics are likely related to the flow pattern transition subjected to heat addition. The location of refrigerant inlet does not significantly affect the performance of heat exchangers.

NOMENCLATURE

D inside diameter of tube
 D_c tube diameter after expansion
 D_o outer diameter of tube
 $F = \sqrt{\frac{\rho_G}{\rho_M - \rho_G}} \frac{V_{VS}}{\sqrt{Dg \cos \beta}}$
 F_p fin pitch
 G mass velocity
 H height of heat exchanger
 i_g latent heat of the liquid refrigerant

N number of tube row
 P pressure
 P_d waffle height of the wavy fin pattern
 P_l longitudinal tube pitch
 P_t transverse tube pitch
 q heat flux
 Q non-dimensional heat input quantity defined in Eq. (1).
 V_f frontal velocity across coil
 V_{VS} the superficial velocity of that portion of gas that flows above the interface.
 $T = \left[\frac{(dP/dx)_{MS}}{(\rho_M - \rho_G)g \cos \beta} \right]^{1/2}$
 T_{sat} saturation temperature
 W width of heat exchanger
 X modified Martinelli parameter,
 $\left[\left(\frac{dP}{dz} \right)_{MS} / \left(\frac{dP}{dz} \right)_{VS} \right]^{1/2}$
 x vapor quality, dimensionless
 z axial length along the direction of evaporator

INTRODUCTION

Plate fin-and-tube heat exchangers are widely used in air-conditioning and refrigeration applications. The heat exchangers are usually composed of mechanically or hydraulically expanded round tubes into a block of parallel continuous fins, and depending on the application, the heat exchangers can be produced in one or more rows.

In practice, refrigerant flows into the heat exchangers may be subdivided into several circuits due to the limitation of pressure drops within the heat exchangers. A good circuit arrangement is very important since it may provide better refrigerant-side distribution; and increase the mean effective temperature difference between the air and refrigerant. Hence, higher heat transfer rates can be achieved. Though multiple circuitry design within the heat exchanger is very common, basic information related to the circuitry design is very rare.

There are some theoretical works related to the present issue. Ellison et al. (1981) proposed an index technique that can efficiently keep track of the refrigerant flow within the circuitry. This technique can handle multiple circuitry and the splitting and dividing of air encountered in fin-and-tube heat exchangers. Kaga et al. (1994) numerically calculated the effect of heat conduction through fins on plate fin-and-tube heat exchangers using a thermal network method. Based on the index technique proposed by Ellison et al. (1981), Liaw and Wang (1998) developed a design program for fin-and-tube evaporators that can account for the effect of complex circuitry.

Converse to the theoretical investigation, experimental data related to the effect of circuitry are very limited. Designs of the circuitry were usually performed based on field experiences. Ebisu et al. (1996) reported performances of air-cooled heat exchangers with R-410A for three different circuits. They reported that the heat exchanger performances for 2 and 3 circuits surpassed that of 1-circuit design by 17% and 19%, respectively. Wang et al. (1999) investigated the effect of circuitry on the performance of air-cooled condensers. They provided in-depth experimental information related to circuitry on the performance of an air-cooled condenser. They found that counter-cross flow would give better performance than other arrangements for 1-circuit arrangements. In addition, a unique feature of "pressure gain" was observed for their results of 2-circuits when one circuit is completely condensed and the other is still in the two-phase region.

As indicated previously, the information about the effect of circuitry on the performance of evaporators is very limited. It is to be noted that when the air flows across the evaporators, moisture is condensed on the fins and water may adhere to the surface as droplets causing bridging between the fins. Accordingly, the effect of circuitry may interact with the airflow and result in much more complex phenomena. The objective of the present study is a continuation of previous effort (Wang et al., 1999), however, focus is made on the basic information about the effect of circuitry within an evaporator.

EXPERIMENTAL APPARATUS

Experiments were performed in an environmental chamber as shown in Figure 1. The test apparatus is based on the air-enthalpy method proposed by ANSI/ASHRAE Standard 37

(1988). The capacity of the evaporator was measured by the enthalpy difference of the airflow across the test sample. The airflow measuring apparatus is constructed based on ASHRAE Standard 41.2 (1987). Refrigerant R-22 was used as the working fluid. The test conditions are as follows:

Air inlet dry-bulb temperature	: 26 ± 0.5 °C
Air inlet wet-bulb temperature	: 20 ± 0.5 °C
Relative humidity	: 60%
Inlet air velocity	: $0.4 \square 1.5$ m/s
Inlet refrigerant temperature	: $11 \square \pm 0.3$ °C
Inlet refrigerant quality	: 0.2 ± 0.03
Inlet refrigerant mass flux	: 100, 200, and 300 kg/s·m ²

A total of six samples of fin-and-tube heat exchangers were made and tested in this study, as shown in Figure 2. Arrangements of (A) and (C) are counter-cross flow, arrangements of (B) and (D) are parallel-cross flow; and arrangements of (E) and (F) are z-shape cross flow. Note that the inlets for arrangements of (A), (B) and (E) are located at the upper portion while the inlets of arrangements of (C), (D), and (F) are located at the lower portion of the test samples. The fin pattern for the present test sample is wavy fin, and the corresponding geometry is given as follows:

Frontal area of the heat exchanger (W×H):	595×305 mm.
Longitudinal tube pitch (P_l):	19.05 mm
Transverse tube pitch (P_t):	25.4 mm
Waffle height (P_w):	1.18 mm.
Fin pitch (F_p):	1.7 mm.
Number of tube row (N):	2
Nominal tube diameter (D_o):	9.52 mm
Tube diameter after expansion (D_e):	10.24 mm
Tube wall thickness:	0.35 mm
Tube configuration:	smooth tube

In order to maintain the inlet state of the refrigerant flow, a refrigerant loop, a heating water flow loop (preheater) and a cooling water loop (subcooler) were provided. The refrigerant flow loop consists of a variable speed gear pump which delivers subcooled refrigerant to the preheater. The refrigerant pump can provide refrigerant mass fluxes ranging from 50 to 400 kg/m²·s. A very accurate mass flowmeter is installed between the refrigerant pump and the preheater. The accuracy of the mass flowmeter is within 0.3% of the test span. The inlet quality was maintained by adjusting the preheater to be 0.2 ± 0.03 . A pressure transducer having 10 Pa resolution was installed to measure the pressure drop across the test heat exchanger. The pressure taps of the test heat exchanger were located 450 mm upstream and downstream of the heat exchangers. Two absolute pressure transducers with resolution up to 0.1 kPa were installed at the inlet and exit of the test section. The water and refrigerant temperatures, were measured by RTDs (Pt100Ω) having a calibrated accuracy of 0.05°C. All the data signals were collected and converted by a data acquisition system (Hybrid recorder). The data acquisition

system then transmits the converted signals through general purpose interface bus to a host computer for further operation. In this study, the physical and transport properties for R-22 were evaluated from a computer program (REFPROP, 1998).

RESULTS AND DISCUSSION

Figure 3 shows the variation of wall temperatures along the refrigerant direction for arrangements (A) to (F) for $G = 100 \text{ kg/m}^2\text{-s}$. As seen in the figure, the exit temperatures for the counter-cross arrangements (A) and (C) are higher than those of parallel-cross flow arrangements (B) and (D). The test results indicated that the location of inlets does not have significant influence on the heat exchanger performance. It is

very interesting to see that the z-shape arrangements of (E) and (F) give the highest exit temperature. The results indicate that the heat transfer performances for the z-shape arrangements outperforms other arrangements. Usually, one would expect the counter-cross arrangement should have the best performance. The results are analogous to those encountered in condensers as explained by Wang et al. (1999). For the present counter-flow arrangement, the inlet and exit portions are close to each other (Fig. 2a). Therefore the temperature at the inlet portion (row 2, upper side) is much lower than that at the exit (row 1, upper side). As a result, larger difference between the adjacent tubes may significantly increase the contribution of the heat conduction along the fin. The reversed heat transfer by heat conduction may offset the benefits of the counter-cross flow arrangement. For the z-shape arrangement (E) or (F), the temperature difference between the neighboring tube is relatively small, therefore reversed heat transfer by conduction is comparatively small.

To explain this phenomenon further, one may have to examine the detailed variations of the wall temperatures along the evaporator as illustrated in Figure 4. For $G = 100 \text{ kg/m}^2\text{-s}$, one can clearly see that arrangement (A) is superior to arrangement (E) since the wall temperature rise for arrangement (A) occurs more quickly than arrangement (E). For instance, the wall temperature for arrangement (A) is approximately 11°C higher than that of arrangement (E) near $z = 6 \text{ m}$. The result substantiates that the counter-cross flow may have a higher heat transfer performance than the z-shape arrangement. However, the wall temperature for arrangement (A) does not consistently increase along the evaporator. Actually, the temperature may even decrease when $z > 8 \text{ m}$ at $G = 100 \text{ kg/m}^2\text{-s}$. Notice that the z-shape arrangement (E) does not show this phenomenon. For $G = 200 \text{ kg/m}^2\text{-s}$, the test results also report similar phenomena. The wall temperatures for arrangement (A) rise more quickly than arrangement (E) but reaches an asymptotic value that is lower than arrangement (E) at the exit.

Figures 5a, 5b, and 5c show the pressure drops on the refrigerant-side vs. frontal velocities for $G = 100, 200$ and $300 \text{ kg/m}^2\text{-s}$. The results indicate that the pressure drop increases with the front velocity. However, as seen in Fig. 5b, there is an exceptional phenomenon for $G = 200 \text{ kg/m}^2\text{-s}$ and parallel flow arrangement. This phenomenon was not seen for $G = 100$ and $300 \text{ kg/m}^2\text{-s}$ and other arrangements. The pressure drop decreases with increase of frontal velocities. We will defer the discussion of this exceptional case later.

Basically, the pressure drop within an evaporator is opposite to the case of an air-cooled condenser where the pressure drop decreases with an increase of the frontal velocity (Wang et al., 1999). This is because both of the accelerational pressure, Δp_a , and frictional pressure Δp_f , increase with the air

velocity. The pressure drop for parallel flow arrangement (D) is usually larger than those of other arrangements for $G = 200 \text{ kg/m}^2\text{-s}$. Note that the present test samples are 2-row configurations. Therefore, for the parallel flow arrangement, it is obvious that the temperature difference between the airflow and the first row is larger than with other arrangements. Hence, the refrigerant moves faster in the first row. Consequently, higher pressure drop is expected owing to the contribution of accelerational pressure. In counter-flow arrangement, the contribution of accelerational pressure is milder in the second row. Therefore, the effective length having a higher quality refrigerant is shorter than those of parallel flow cases. Thus, for the same mass flux, the pressure drop for parallel flow arrangement is usually larger than those of other arrangements.

However, as shown in Fig. 5b, for $G = 200 \text{ kg/m}^2\text{-s}$ and parallel flow arrangement, the pressure drop decreases with the frontal velocity. This phenomenon is not seen for $G = 100$ and $300 \text{ kg/m}^2\text{-s}$ of parallel flow arrangement, nor for counter-flow and z-shape arrangements. This phenomenon is related to change of two-phase flow patterns.

As pointed out by Wang et al. (1997) in a two-phase flow pattern visualization having refrigerants R-22, R-134a, and R-407C in a 6.5-mm smooth tube, they reported that for $G = 100 \text{ kg/m}^2\text{-s}$, the major flow pattern in a 6.5-mm tube is stratified flow, no annular flow pattern is observed; for $G = 200 \text{ kg/m}^2\text{-s}$, the flow patterns are intermittent (quality, $x < 0.2$), stratified, and annular ($x > 0.6$); for $G = 400 \text{ kg/m}^2\text{-s}$, the major flow pattern is annular. Although the inside diameter (about 9.2 mm) of the present sample is slightly different from that of Wang et al. (1997), it is likely that the two-phase flow pattern in the present test samples is analogous to those of 6.5 mm. Therefore, for the present test results of $G = 100$ and $300 \text{ kg/m}^2\text{-s}$, the major flow patterns may be stratified and annular flow pattern since the quality into the test samples is about 0.2. Hence,

drop should increase with the frontal velocities owing to the contribution of acceleration.

To explain the phenomenon that the pressure drop decreases with frontal velocities for parallel flow and $G = 200 \text{ kg/m}^2\text{-s}$, one may look into the effect of heat flux on the transition of the flow pattern. Notice that the above results by Wang et al. (1997) were for adiabatic two-phase flow, the application of diabatic flow patterns is somewhat different from adiabatic flow. This is because in boiling flow the voids increase along the tube, and the flow patterns vary accordingly. Dukler and Taitel (1991) presented a generalized coordinate map for horizontal tubes for a boiling case using a dimensionless heat transfer parameter, Q , defined as

$$Q = \frac{q \pi V_{VS}}{i_{fg} D (dP/dz)_{VS}} \quad (1)$$

Figure 6 is a schematic of change of flow pattern subjected to heat addition. This flow pattern map is based on the famous map proposed by Taitel and Dukler (1976). As seen in Fig. 6, with heat addition, the transition from stratified flow to annular flow may be delayed. This phenomenon may become pronounced with higher Q . For parallel flow arrangement, it is obvious that the effect of Q is much more pronounced since the temperature difference is much larger than that for other arrangements in the first row. Consequently, as depicted in Fig. 6, the transition from stratified flow to annular flow may be further delayed with increase of frontal velocities (Note that for air-cooled heat exchangers, the dominant resistance is on the airside. Therefore Q increases with increase of frontal velocities). The pressure drop for annular flow pattern case is expected to be higher than those in stratified flow. In this connection, the pressure drop may decrease with increase of frontal velocities. For $G = 100$ and $300 \text{ kg/m}^2\text{-s}$, as shown in Figure 6, there may not be a significant change of flow pattern. Therefore the pressure drop does not reveal unusual characteristics. For $G = 200/\text{m}^2\text{-s}$ and other arrangements, the effect of Q on the flow pattern transition is not as pronounced as parallel flow. This is because the temperature difference between the airflow and the first row (or the second row) is smaller. Furthermore, for the first row in the counter-flow arrangement, the flow pattern may already develop into

- The counter-cross arrangement gives better performance. However, the reversed heat conduction from the inlet portion to the exit portion may offset the benefit of counter-cross arrangement.
- The refrigerant-side pressure drop for parallel flow is usually higher than those of other arrangements.
- The pressure drop on the refrigerant-side was increased with the frontal velocity across the evaporator (except for $G = 200/\text{m}^2\text{-s}$ and parallel flow). The phenomenon is opposite to the case of an air-cooled condenser that the pressure drop decreases with the frontal velocity.
- For $G = 200 \text{ kg/m}^2\text{-s}$ and parallel flow arrangement, the pressure drop decreases with increase of frontal velocities. It is very likely that this unusual phenomenon is related to the transition of flow pattern subjected to heat addition.

ACKNOWLEDGMENTS

The authors would like to express gratitude for the Energy Research and Information funding from the Energy Commission of the Ministry of Economic Affairs, which provided the financial support for the current study.

REFERENCES

- ANSI/ASHRAE Standard 37, 1988, "Methods of Testing for Rating Unitary Air-conditioning and Heat Pump Equipment".
- ASHRAE Standard 41-2, 1987, "Standard Methods for Laboratory Air-flow Measurement".
- Dukler, A.E., and Taitel, Y., 1991, "Flow patterns transitions in Gas-Liquid Systems," chap. 3 in *Two-phase Gas-Liquid Flow: A short course on principles of Modeling Gas-Liquid Flow and on Modern Measuring Methods*, University of Houston, Houston. This paper is quoted from the chapter 3 of the monograph by Tong and Tang, *Boiling Heat Transfer and Two-phase Flow*, 1997, Taylor & Francis.
- Ebisu, T., Yoshida, K., and Torikoshi, K., 1996, "Air-cooled Heat Exchanger Performance for R-410A", Proceedings of 1996 *International Refrigerant Conf.* Purdue, USA, pp.139-144.

10th Int. heat Transfer Conf., Brayton, UK, the industrial sections paper, paper no. I/2-CHE-8 99-104, pp. 99-104.

Liaw J.S., and Wang, C.C. 1998, "A Computer Model for Evaporator; Accounting the Effect of Complex Circuitry," Proceedings of the 11th Int. Symposium on Transport Phenomena, Hsinchu, Taiwan, pp. 138-143.

REFPROP 6.0, Gaithersburg, 1998, MD: National Institute of Standards and Technology.

Taitel, Y., and Dukler, A.E., 1976, "A Model for Prediction of Flow Regime Transitions in Horizontal and Near Horizontal Gas-liquid Flow," *AIChE J*, Vol. 22, pp. 47-55.

Wang, C. C., Chiang, C. S., and Lu, D. C., 1997, "Visual Observation of Flow Pattern of R-22, R-134a, and R-407C in a 6.5 mm Smooth Tube," *Experimental Thermal and Fluid Science*, Vol. 15, no. 4, pp.395-405.

Wang C.C., Jang J.Y., Lai C.C., Chang Y.J., 1999, "Effect of circuit arrangement on the performance of air-cooled condensers," *International Journal of Refrigeration*, Vol. 22, pp. 275-282.

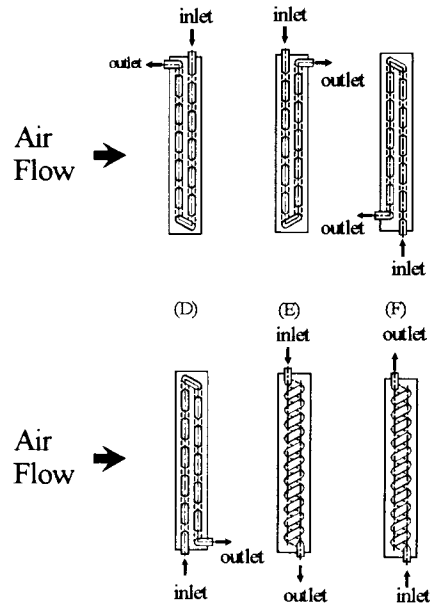


Figure 2 Schematic of the 1-circuit arrangement tested in this study.

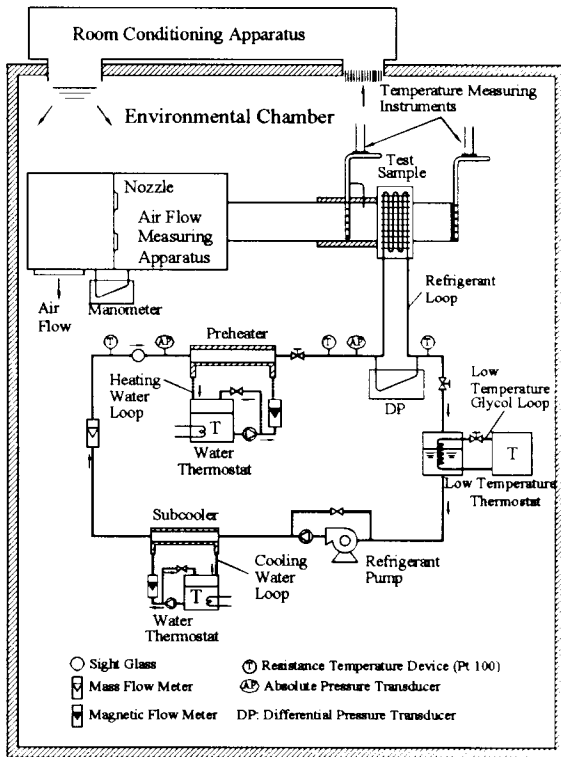


Figure 1 Schematic of experimental setup.

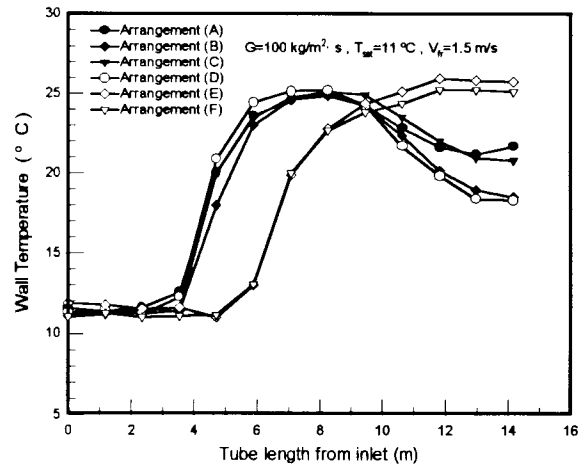


Figure 3 Wall temperature variations for arrangements (A) through (F) at $V_{fr} = 1.5 \text{ m/s}$ and $G = 100 \text{ kg/m}^2 \cdot \text{s}$.

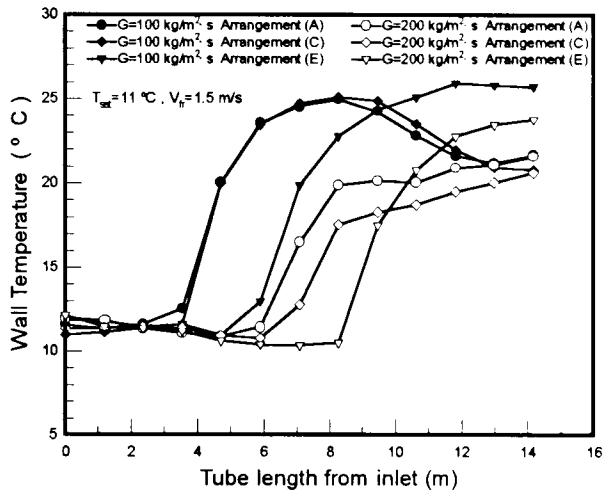


Figure 4 Wall temperature variations for arrangements (A), (C) and (E) at $V_{fr} = 1.5$ m/s and $G = 100, 200$ kg/m²·s.

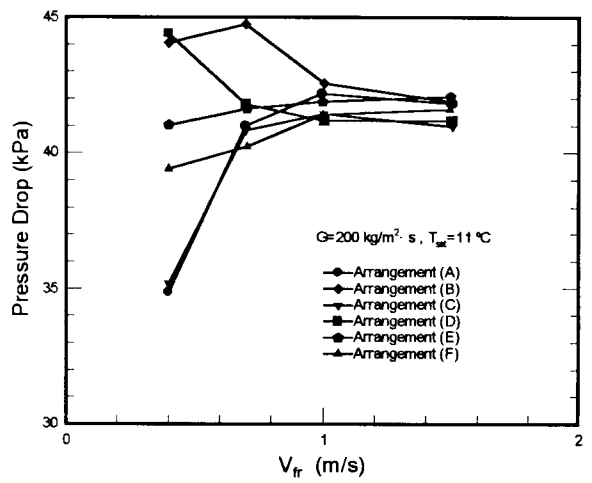


Figure 5b Pressure drops vs. frontal velocity for arrangements (A)..(F) at $G = 200$ kg/m²·s.

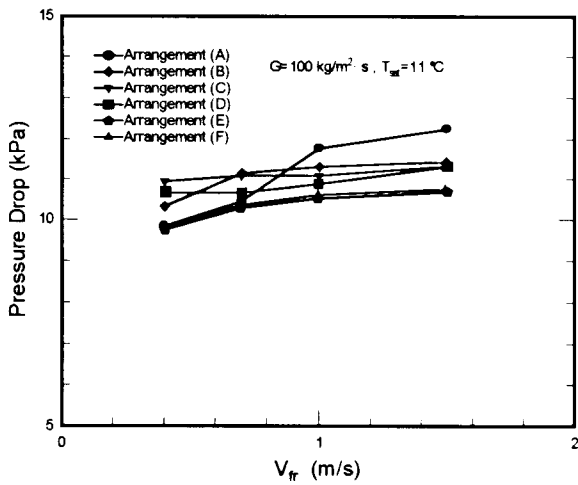


Figure 5a Pressure drops vs. frontal velocity for arrangements (A)..(F) at $G = 100$ kg/m²·s.

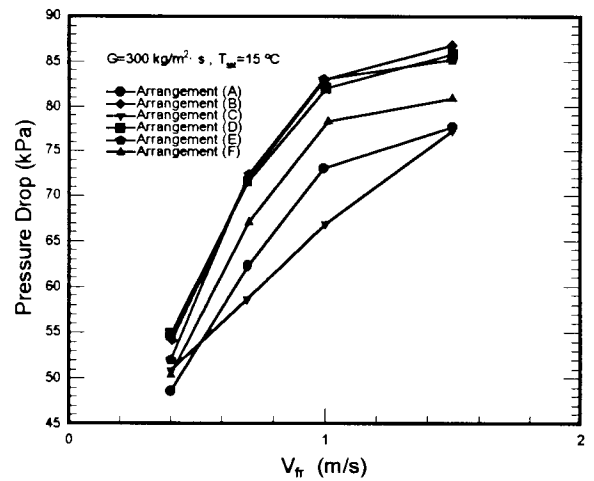
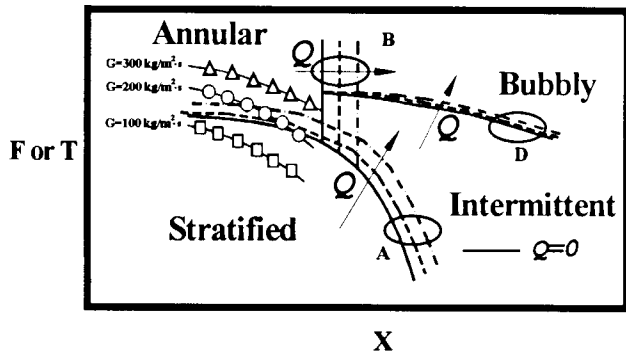


Figure 5c Pressure drops vs. frontal velocity for arrangements (A)..(F) at $G = 300$ kg/m²·s.



CURVES	A&B	D
COORDINATES	F vs X	T vs X

Figure 6 Schematic of the flow pattern transition for adiabatic flow.